



A selenolactone-based fluorescent chemodosimeter to monitor mercury/methylmercury species *in vitro* and *in vivo*

Xiaoqiang Chen^{a,d,†}, Kyung-Hwa Baek^{b,†}, Youngmee Kim^a, Sung-Jin Kim^a,
Injae Shin^{b,*}, Juyoung Yoon^{a,c,*}

^a Department of Chemistry and Nano Science, Ewha Womans University, Seoul 120-750, Republic of Korea

^b Center for Biofunctional Molecules, Department of Chemistry, Yonsei University, Seoul 120-749, Republic of Korea

^c Department of Bioinspired Science, Ewha Womans University, Seoul 120-750, Republic of Korea

^d State Key Laboratory of Materials-Oriented Chemical Engineering, College of Chemistry and Chemical Engineering, Nanjing University of Technology, Nanjing 210009, China

ARTICLE INFO

Article history:

Received 16 March 2010

Received in revised form

9 April 2010

Accepted 10 April 2010

Keywords:

Fluorescent chemodosimeter

Selenolactone

Rhodamine

Mercury

Methylmercury

ABSTRACT

A fluorescent probe based on selenolactone displays unique fluorescence enhancement and UV–vis spectral change for mercury/methylmercury species, which were attributed to deselenation reaction. The value of this system was successfully demonstrated by its use in detecting inorganic mercury/methylmercury species in cells and zebrafish.

© 2010 Elsevier Ltd. All rights reserved.

1. Introduction

Mercury exists in the environment as inorganic and organic mercury species.¹ Inorganic mercury is one of the most prevalent toxic metals in the environment, and gains access to the body orally or dermally. When absorbed in the human body, these species result in damage to the brain, kidneys, and endocrine system. On the other hand, inorganic mercury, released into the environment through a variety of anthropogenic and natural sources, can be converted to organomercury mainly through methylation by aquatic microorganisms.² Organic forms of mercury are much more toxic than inorganic mercury species since they can readily pass through biological membranes.³ Exposure of methylmercury, a typical organic mercury, to the human body causes cardiovascular diseases, autoimmune effects, hearing impairment, blindness, and death.^{3a} Therefore, the detection of inorganic and organic mercury species is of great interest in the aspect of both environment and human health.

* Corresponding authors. Tel.: +82 2 3277 2400; fax: +82 2 3277 3419 (J.Y.); tel.: +82 2 2123 2631; fax: 82 2 364 7050 (I.S.); e-mail addresses: injae@yonsei.ac.kr (I.Shin), jyoon@ewha.ac.kr (J.Yoon).

[†] Equally contributed to this work.

Typical analytical methods, such as atomic absorption spectroscopy, cold vapor atomic fluorescence spectrometry, gas chromatography, and high performance liquid chromatography, have been employed to monitor mercury species.¹ However, many of these methods require complicated, multistep sample preparation, and sophisticated instrumentation. As a consequence, convenient and simple methods based on optical detection, such as fluorescence or colorimetric changes are preferable.⁴ As part of this effort, a variety of fluorescent probes for the detection of mercury species with ease and high sensitivity have recently been exploited.^{1,5} Surprisingly, most of these probes only sense inorganic mercury ions and chemosensors to detect methylmercury species are rare.⁶

Rhodamine derivatives have received increasing attention in designing chemosensors for metal ions.⁷ If rhodamine derivatives contain a spiro ring system, they are non-fluorescent and colorless. However, when the spiro rings in rhodamine derivatives are opened by stimulus, they exhibit strong fluorescence emission and a pink color. Owing to the extremely high affinity between mercury and selenium, we design here a fluorescent chemodosimeter based on rhodamine B selenolactone for inorganic mercury and methylmercury species. During the preparation our manuscript, the titled molecular has been reported as inorganic mercury and silver sensor by Ma et al.⁸

However, in our work, we demonstrated the probe can also detect methylmercury species, and describe its application for *in vitro* and *in vivo* monitoring of inorganic and organic mercury species.

2. Results and discussion

2.1. Synthesis and X-ray crystal structure

The designed fluorescent probe **1** was prepared by reacting rhodamine B with phosphorous oxychloride in 1,2-dichloroethane under reflux, followed by reaction with selenourea in 20 mM HEPES buffer (pH 7.4, 1% CH₃CN). The crude product was purified by silica-gel column chromatography with CH₂Cl₂ as eluent to afford **1** in 37% yield. The detailed experimental procedures and spectral data are provided in [Experimental section](#) and [Supplementary data](#). The structure of a probe **1** was also confirmed by X-ray analysis of its single crystal that was grown in acetonitrile. A unique seleno-lactone structure was observed as shown in [Figure 1b](#).

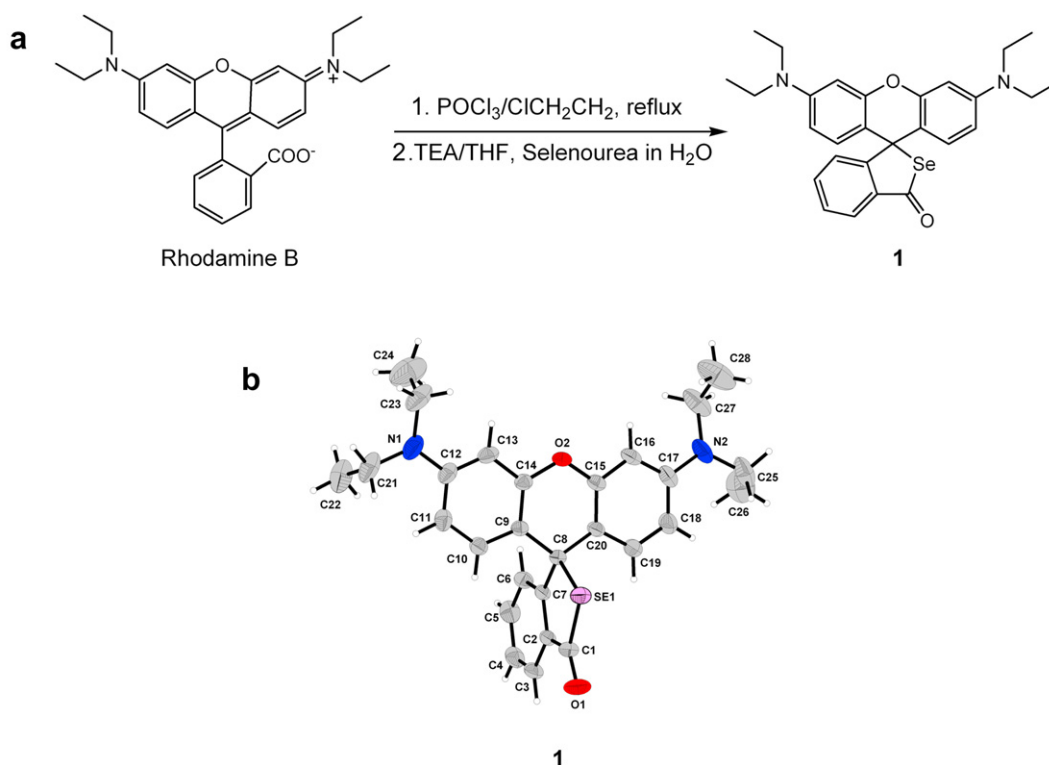


Figure 1. a) Synthesis of a fluorescent probe **1** and (b) its X-ray crystal structure.

2.2. Optical change of **1** with Hg²⁺ and its proposed mechanism

Initially, selective response of **1** to metal ions was examined. For this study, a probe **1** (10 μM) was treated with various metal ions (100 μM), such as Cu²⁺, Ni²⁺, Zn²⁺, Cd²⁺, Co²⁺, Cs⁺, Li⁺, Ca²⁺, Mn²⁺, K⁺, Na⁺, Sr²⁺, Fe²⁺, Al³⁺, Mg²⁺, Pb²⁺, Fe³⁺, Ag⁺, and Hg²⁺ ions in 20 mM HEPES buffer (pH 7.4, 1% CH₃CN). UV–vis and fluorescence spectra reveal that a probe **1** is non-fluorescent in aqueous solution and selectively responds to Hg²⁺ among the various metal ions examined ([Fig. 2](#) and [Supplementary data, Fig. S1](#)). As large as 30-fold ‘off-on’ type fluorescence enhancement was observed upon the addition of 10 equiv of Hg²⁺ ([Fig. 2](#)). As shown in [Figure 3](#), there was also a large enhancement in the UV absorption (λ_{max}=560 nm)

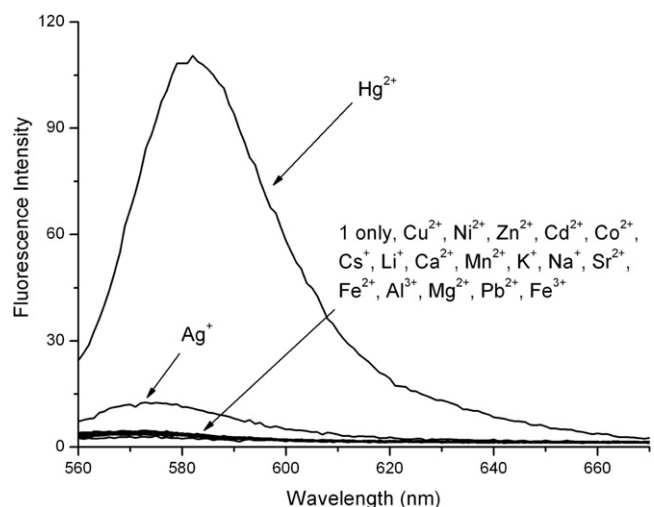


Figure 2. Fluorescence spectra of **1** (10 μM) with metal ions (100 μM) in 20 mM HEPES buffer (pH 7.4, 1% CH₃CN) (λ_{ex}=550 nm).

of a probe **1** upon the addition of Hg²⁺. The Hg²⁺ concentration-dependent absorption spectra of **1** at 560 nm indicated that saturation reaches after addition of 1 equiv of Hg²⁺. Colorless to pink color change was also observed after treatment of **1** with Hg²⁺ ([Supplementary data, Fig. S2](#)). The stoichiometry of a binding event between Hg²⁺ and **1** was also determined. The results obtained from Job’s plot show the 1:1 stoichiometry between **1** and Hg²⁺ ([Supplementary data, Fig. S3](#)).

On the detection mechanism, the Hg²⁺-induced spiro ring opening of rhodamine followed by deselenation is likely to be responsible for the fluorescence enhancement and UV–vis spectral change ([Scheme 1](#)). To examine this plausible mechanism, a product obtained from the reaction of **1** with Hg(ClO₄)₂ was analyzed. According to MS analysis, a peak at 433.23 corresponding to

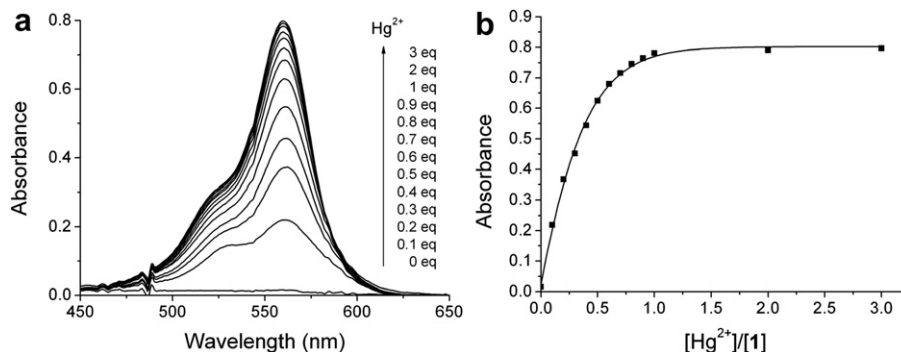
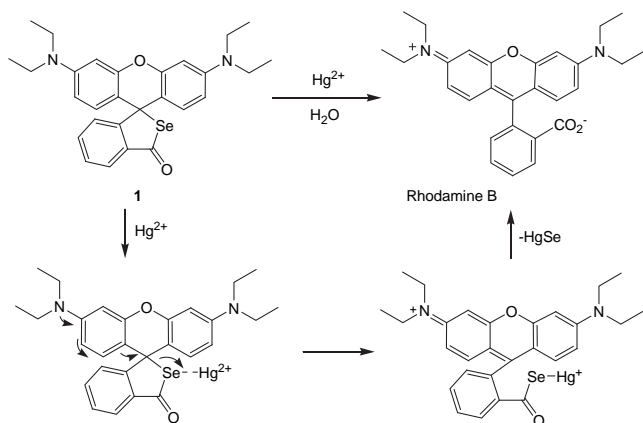


Figure 3. (a) Absorption spectra of **1** (10 μM) in the presence of various concentrations of Hg^{2+} (0, 0.1, 2, 3, 4, 5, 6, 7, 8, 9, 10, 20, 30 μM) in 20 mM HEPES buffer (pH 7.4, 1% CH_3CN). (b) Hg^{2+} concentration-dependent absorbance of **1**. Absorbance of **1** (10 μM) was measured at 560 nm in the presence of various amounts of Hg^{2+} . Each spectrum is recorded at 5 min after addition of Hg^{2+} to **1**.



Scheme 1. A plausible mechanism of deselenation of **1** by mercury ions.

[rhodamine B+H]⁺ was clearly observed, suggesting the formation of rhodamine B (Supplementary data, Fig. S4). NMR spectroscopic analysis also provided the evidence for deselenation of **1** by Hg^{2+} (Supplementary data, Fig. S5).

To investigate detection limit of **1** for Hg^{2+} , **1** (1 μM) was treated with various concentrations of Hg^{2+} (0–30 nM). The fluorescence intensity at 580 nm was plotted as a function of the Hg^{2+} concentration (Supplementary data, Fig. S6). The fluorescence intensity of **1** is linearly proportional to the Hg^{2+} concentration of 0–30 nM, and as low as 20 nM concentration of Hg^{2+} was detected by using **1** with a signal-to-noise ratio of 3. The time-dependent fluorescence response of **1** to Hg^{2+} was monitored at 580 nm under pseudo-first-order kinetic conditions (10 μM **1** and 500 μM Hg^{2+}). Under these conditions, the observed rate constant (k_{obs}) at pH 7.4 was found to be 0.14 min^{-1} for Hg^{2+} (Supplementary data,

Fig. S7). Furthermore, we investigated potential interference of fluorescence response of **1** to mercury ions from various metal ions. The results obtained from fluorescence experiments show that **1** retains high selectivity for Hg^{2+} in the presence of millimolar concentrations of various metal ions including Li^+ , Na^+ , K^+ , Ca^{2+} , Mg^{2+} , Cd^{2+} , Co^{2+} , Cu^{2+} , Fe^{2+} , Mn^{2+} , Ni^{2+} , Pb^{2+} , and Zn^{2+} (Supplementary data, Fig. S8).

2.3. Optical change of **1** with methylmercury and its proposed mechanism

It should be more significant to monitor methylmercury species using **1** because organic forms of mercury are more toxic than inorganic mercury species. For this study, **1** (10 μM) was treated with various concentrations (0–100 μM) of CH_3HgCl in 20 mM HEPES buffer (pH 7.4, 1% CH_3CN). Similar UV–vis and fluorescence spectra to those on inorganic mercury were obtained (Fig. 4). A absorption band centered at 560 nm appeared with increasing intensity, which induced a clear color change from colorless to pink color. In addition, an emissive peak at 580 nm was observed in the presence of the CH_3HgCl . After addition of 10 equiv methyl mercury to the solution with sensor for various reaction times, the results show the enhancement of fluorescence intensity can be completed in 10 min (Supplementary data, Fig. S9). Both UV–vis and fluorescence data lead to a significant ‘off-on’ signal. Two peaks can be observed from the mass spectra of **1** upon the addition of CH_3HgCl (10 equiv), corresponding to [rhodamine B+H]⁺ and [1-HgCH₃]⁺, indicating that the mechanism of reaction between **1** and CH_3HgCl is similar with the case of Hg^{2+} . In the procedure of reaction between **1** and CH_3HgCl , **1** initially bind with CH_3HgCl and the following deselenation of 1-HgCH₃ happen, so both the peaks of [1-HgCH₃]⁺ and [rhodamine B+H]⁺ can be observed from mass spectra (Supplementary data, Fig. S10).

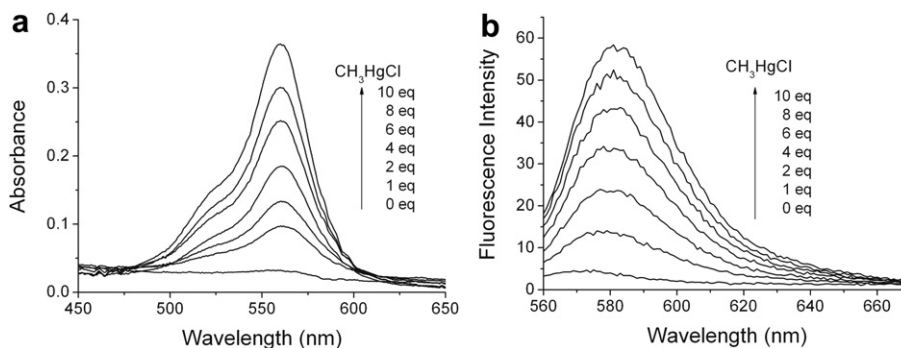


Figure 4. (a) Absorption spectra of **1** (10 μM) in the presence of various concentrations of CH_3HgCl (0, 10, 20, 40, 60, 80, 100 μM) in 20 mM HEPES buffer (pH 7.4, 1% CH_3CN). (b) Fluorescence spectra of **1** (10 μM) in the presence of various concentrations of CH_3HgCl (0, 10, 20, 40, 60, 80, 100 μM) in 20 mM HEPES buffer (pH 7.4, 1% CH_3CN) ($\lambda_{\text{ex}}=550$ nm).

2.4. Sensing inorganic mercury and methylmercury in the cell as well as in the zebra fish

Owing to its chemical and spectroscopic properties, **1** should be suited to monitoring inorganic mercury and methylmercury in living cells. To test this proposal, HeLa cells (human epithelial adenocarcinoma) were incubated with **1** (20 μM) in the culture media (0.2% DMSO). In the absence of mercury ions or methylmercury, no fluorescence was exhibited inside the cells (Fig. 5a). However, when the cells were treated with **1** (20 μM) and mercury ions or methylmercury (each 40 μM), a remarkable increase in fluorescence intensity was observed, indicating the detection of inorganic mercury ions and methylmercury by **1** in cells (Fig. 5b and c).

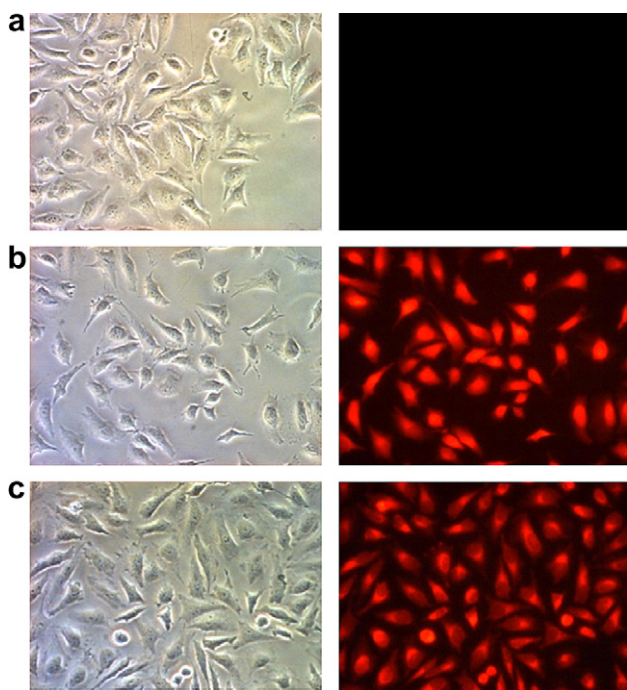


Figure 5. Images of cells incubated with 20 μM **1** (0.2% DMSO) and 40 μM HgCl_2 or 40 μM CH_3HgCl . (a) Images of HeLa cells treated with **1** in the absence, (b) presence of 40 μM HgCl_2 and (c) presence of 40 μM CH_3HgCl (left, light microscopic images; right, fluorescence images).

We then made attempt to monitor the mercury species accumulated in living organisms using **1**. Zebrafish is a good animal model to monitor ions using sensors due to convenient detection of ions by fluorescence microscopy and permeability of ions and sensors in fish.⁹ For this study, adult zebrafish (three months old with identifiable organs) was pre-incubated with 500 nM mercury ions or 500 nM methylmercury in water for 24 h (Fig. 6). And then the treated zebrafish was further exposed to 20 mM of **1** for 1 h. Zebrafish was dissected to isolate tissues and organs that were examined using fluorescence microscopy. Inorganic mercury and methylmercury species were detected in the gall-bladder, eggs and fin, and weakly monitored in gills and heart by **1**. The results obtained from cell and zebrafish experiments show that **1** can pass through cells and fish, and then reacts with HgCl_2 or CH_3HgCl to form the fluorescent product.

3. Conclusions

In summary, we have developed a new selenolactone-based fluorescent probe for the detection of inorganic mercury and

methylmercury species with high selectivity and sensitivity. The fluorescence enhancement and UV–vis spectral change induced by mercury ions are attributed to deselenation reaction. The value of this system was successfully demonstrated by its use in detecting inorganic mercury/methylmercury species in cells and zebrafish.

4. Experimental

4.1. General methods

Unless otherwise noted, materials were obtained from commercial suppliers and were used without further purification. Chromatography was carried out on silica gel 60 (230–400 mesh ASTM; Merck). Thin layer chromatography (TLC) was carried out using Merck 60 F₂₅₄ plates with a thickness of 0.25 mm. Preparative TLC was performed using Merck 60 F₂₅₄ plates with a thickness of 1 mm. ¹H NMR and ¹³C NMR spectra were recorded using Bruker 250. Mass spectra were obtained using a Jeol JMS 700 high resolution mass spectrometer. UV absorption spectra were obtained on UVIKON 933 Double Beam UV/VIS Spectrometer. Fluorescence emission spectra were obtained using RF-5301/PC Spectrofluorophotometer (Shimadzu).

4.2. Preparation of stock solutions for fluorescent/UV–vis study

Stock solutions (10 mM) of the perchlorate salts of metal ions and methylmercury in distilled water were prepared. Stock solutions of **1** (1 mM) were also prepared in acetonitrile. In a typical experiment, test solutions were prepared by placing 30 μL of the probe stock solution into a test tube, diluting the solution to 3 mL with 0.02 M HEPES (pH 7.4), and adding an appropriate buffer of each analytes stock. Normally, excitation was at 550 nm. Both the excitation and emission slit widths were 1.5 nm/1.5 nm. Fluorescence spectra were measured after addition of analytes for 10 min. For low concentration titration of Hg^{2+} , fluorescence spectra were measured after addition of Hg^{2+} for 10 min, and both the excitation and emission slit widths were 3 nm, respectively. Similarly, for concentration titration of CH_3HgCl , fluorescence/UV–vis absorption spectra were measured after addition of CH_3HgCl for 10 min.

4.3. Synthesis of compound **1**

To a stirred solution of rhodamine B (1 g, 2.2 mmol) in 1,2-dichloroethane (10 mL), phosphorus oxychloride (2 mL) was added dropwise. After refluxed for 4 h, the reaction mixture was cooled and evaporated in vacuo. The crude acid chloride was dissolved in THF (6 mL), and the resulting solution was then added dropwise to a mixed solution of selenourea (500 mg, 4.1 mmol) and triethylamine (6 mL) in THF (25 mL)/water (5 mL) at room temperature. After stirring over night, the solvent was removed under reduced pressure. Then, 30 mL of water was added, and the formed precipitate was filtered. The precipitate was washed several times with water and dried. The crude product was purified by silica-gel column chromatography with CH_2Cl_2 as eluent, affording 0.410 mg of **1** in 37% yield. ¹H NMR (CDCl_3 , 250 MHz) δ (ppm): 7.79 (d, ¹H, $J=6.9$ Hz), 7.46–7.34 (m, 2H), 7.18 (d, 1H, $J=6.6$ Hz), 6.62 (d, 2H, $J=8.3$ Hz), 6.24 (s, 2H), 6.20 (d, 2H, $J=8.5$ Hz), 3.26 (q, 8H, $J=7.0$ Hz), 1.08 (t, 12H, $J=7.0$ Hz). ¹³C NMR (CDCl_3 , 62.5 MHz) δ (ppm): 201.688, 158.732, 152.283, 148.191, 140.878, 134.121, 130.090, 128.418, 128.158, 122.522, 110.957, 108.130, 97.449, 62.725, 44.371, 12.634. FABMS $m/z=507.1548$ [$\text{M}+\text{H}$]⁺, calcd for $\text{C}_{28}\text{H}_{31}\text{N}_2\text{O}_2\text{Se}=507.1553$.

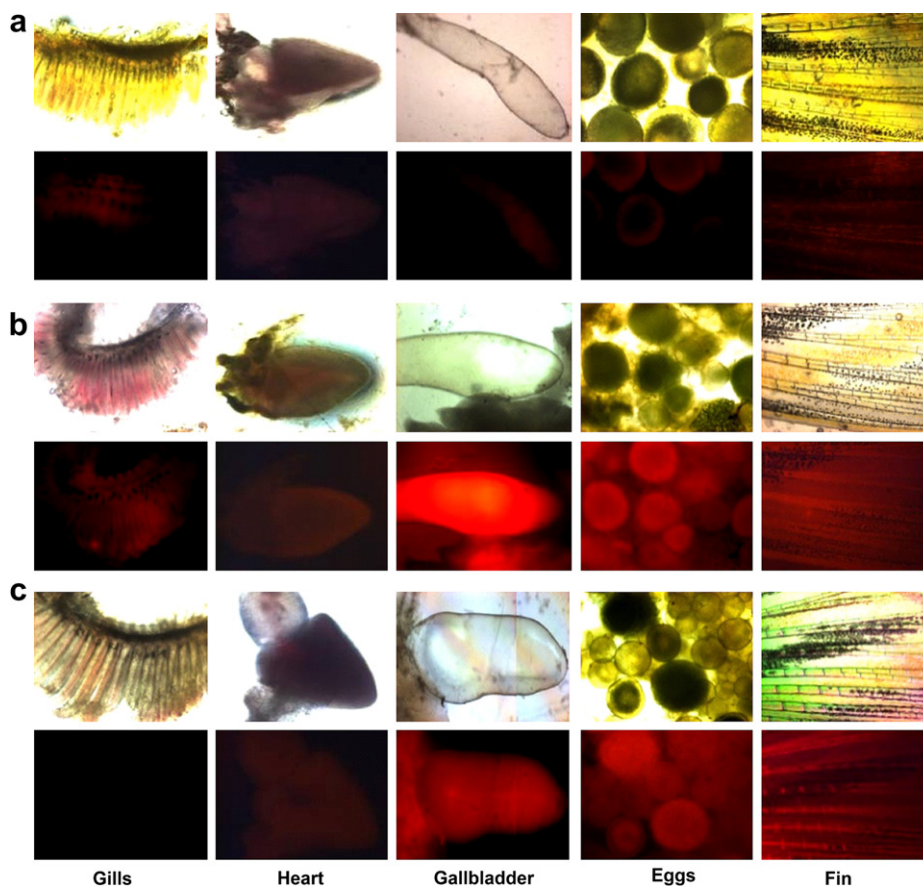


Figure 6. Images of zebrafish organs treated with 20 μM **1** (0.2% DMSO) and 500 nM HgCl_2 or 500 nM CH_3HgCl . (a) Images of zebrafish organs treated with **1** in the absence of HgCl_2 or CH_3HgCl , (b) presence of 500 nM HgCl_2 or (c) presence of 500 nM CH_3HgCl (upper, microscopic images; lower, fluorescence images).

4.4. Imaging of mammalian cells incubated with probe and HgCl_2 or CH_3HgCl

HeLa cells (human epithelial adenocarcinoma) were seeded in a 24-well plate at a density of 2×10^3 cells per well in culture media (RPMI-1640 supplemented with 10% fetal bovine serum (FBS)). After 24 h, 20 μM **1** in the culture media (0.2% DMSO) was added to the cells and the cells were incubated for 1 h at 37 $^\circ\text{C}$. After washing twice with the 400 μL of Dulbecco's phosphate buffered saline (DPBS, without calcium and magnesium) to remove the remaining probe, the cells were further treated with 40 μM HgCl_2 or 40 μM CH_3HgCl in DPBS for 10 min. The treated cells imaged by fluorescence microscopy (Excitation at 510–560 nm, emission at 590 nm, Eclipse TE200-S, Nikon, Japan).

4.5. Detection of mercury ion or CH_3HgCl -containing zebrafish organs incubated with the probe

Adult zebrafish (three-month-old with identifiable organs) was pre-incubated with 500 nM HgCl_2 or 500 nM CH_3HgCl in water for 24 h. After washing twice with water to remove the remaining ions, the zebrafish was further incubated with 20 μM **1** in the water for 1 h at 28 $^\circ\text{C}$. The treated zebrafish was dissected to isolate tissues and organs that were then examined by using fluorescence microscopy (excitation at 510–560 nm, emission at 590 nm, Eclipse TE200-S, Nikon, Japan).

Acknowledgements

This work was supported by grants from the Korea Research Foundation Grant (KRF-2006-005-J04002), the National Research

Foundation of Korea (NRF) (20090083065), the National Creative Research Initiative and WCU (R32-2008-000-10217-0) programs. Mass spectra data were obtained from the Korea Basic Science Institute (Daegu) on a Jeol JMS 700 high resolution mass spectrometer.

Supplementary data

Experimental details, Synthesis and characterization of sensor **1**; UV–vis spectra of **1** with various metal ions; The detection limit assays; Competition experiments and the determination of rate constant; The job-plot of sensor **1** with Hg^{2+} ; ^1H NMR and mass spectra of sensor **1** upon the addition of Hg^{2+} ; Mass spectra of sensor **1** upon the addition of CH_3HgCl . Supplementary data associated with this article can be found in online version at doi:10.1016/j.tet.2010.04.042.

References and notes

- Nolan, E. M.; Lippard, S. J. *Chem. Rev.* **2008**, *108*, 3443.
- (a) Jensen, S.; Jernelov, A. *Nature* **1969**, *223*, 753; (b) Celso, V.; Lean, D. R. S.; Scott, S. L. *Sci. Total Environ.* **2006**, *368*, 126.
- (a) *ATSDR, Toxicological Profile for Mercury*; U.S. Department of Health and Human Services: Atlanta, GA, 1999; (b) *ATSDR, ToxProfiles: Mercury*; U.S. Department of Health and Human Services: Atlanta, GA, 2005; (c) Harada, M. *Crit. Rev. Toxicol.* **1995**, *25*, 1; (d) Mottet, N. K.; Vahter, M. E.; Charleston, J. S.; Friberg, L. T. *Met. Ions Biol. Syst.* **1997**, *34*, 371; (e) Davidson, P. W.; Myers, G. L.; Cox, C.; Axtell, C.; Shamlaye, C.; Sloane-Reeves, J.; Cernichiary, E.; Needham, L.; Choi, A.; Wang, Y.; Berlin, M.; Clarkson, T. W. *JAMA, J. Am. Med. Assoc.* **1998**, *280*, 701; (f) Clarkson, T. W.; Magos, L.; Myers, G. J. *N. Engl. J. Med.* **2003**, *349*, 1731.
- (a) Callan, J. F.; de Silva, A. P.; Magri, D. C. *Tetrahedron* **2005**, *61*, 8551; (b) de Silva, A. P.; Gunaratne, H. Q. N.; Gunnlaugsson, T. A.; Huxley, T. M.; McCoy, C. P.; Rademacher, J. T.; Rice, T. E. *Chem. Rev.* **1997**, *97*, 1515; (c) Czarnik, A. W. *Acc. Chem. Res.* **1994**, *27*, 302; (d) Kim, S. K.; Lee, D. H.; Hong, J.-I.; Yoon, J. *Acc. Chem. Res.* **2009**, *42*, 23; (e) Xu, Z.; Chen, X.; Kim, H. N.; Yoon, J. *Chem. Soc. Rev.* **2010**, *39*, 127;

- (f) Chen, X.; Kang, S.; Kim, M. J.; Kim, J.; Kim, Y. S.; Kim, H.; Chi, B.; Kim, S.-J.; Lee, J. Y.; Yoon, J. *Angew. Chem., Int. Ed.* **2010**, *49*, 1422.
5. (a) Kwon, J. Y.; Soh, J. H.; Yoon, Y. J.; Yoon, J. *Supramol. Chem.* **2004**, *16*, 621; (b) Yang, Y.-K.; Yook, K.-J.; Tae, J. *J. Am. Chem. Soc.* **2005**, *127*, 16760; (c) Liu, B.; Tian, H. *Chem. Commun.* **2005**, 3156; (d) Ros-Lis, J.; Marcos, M. D.; Martínez-Mañez, R.; Rurack, K.; Soto, J. *Angew. Chem., Int. Ed.* **2005**, *44*, 4405; (e) Song, K. C.; Kim, J. S.; Park, S. M.; Chung, K.-C.; Ahn, S.; Chang, S.-K. *Org. Lett.* **2006**, *8*, 3413; (f) Lee, M. H.; Cho, B.-K.; Yoon, J.; Kim, J. S. *Org. Lett.* **2007**, *9*, 4515; (g) Zhang, G.; Zhang, D.; Yin, S.; Yang, X.; Shuai, Z.; Zhu, D. *Chem. Commun.* **2005**, 2161; (h) Shi, W.; Ma, H. *Chem. Commun.* **2008**, 1856; (i) Zhan, X.-Q.; Qian, Z.-H.; Zheng, H.; Su, B.-Y.; Lan, Z.; Xu, J.-G. *Chem. Commun.* **2008**, 1859; (j) Chen, X.; Nam, S.-W.; Jou, M. J.; Kim, Y.; Kim, S.-J.; Park, S.; Yoon, J. *Org. Lett.* **2008**, *10*, 5235; (k) Li, H.-W.; Li, Y.; Dang, Y.-Q.; Ma, L.-J.; Wu, Y.; Hou, G.; Wu, L. *Chem. Commun.* **2009**, 4453; (l) Guo, W.; Yuan, J.; Wang, E. *Chem. Commun.* **2009**, 3395; (m) Huang, W.; Song, C.; He, C.; Lv, G.; Hu, X.; Zhu, X.; Duan, C. *Inorg. Chem.* **2009**, *48*, 5061; (n) Ma, L.-J.; Li, Y.; Li, L.; Sun, J.; Tian, C.; Wu, Y. *Chem. Commun.* **2008**, 6345; (o) Lee, M. H.; Lee, S. W.; Kim, S. H.; Kang, C.; Kim, J. S. *Org. Lett.* **2009**, *11*, 2101; (p) Choi, M. G.; Kim, Y. H.; Namgoong, J. E.; Chang, S.-K. *Chem. Commun.* **2009**, 3560; (q) Soh, J. H.; Swamy, K. M. K.; Kim, S. K.; Kim, S.; Lee, S.-H.; Yoon, J. *Tetrahedron Lett.* **2007**, *48*, 5966; (r) Kwon, S. K.; Kim, H. N.; Rho, J. H.; Swamy, K. M. K.; Shanthakumar, S. M.; Yoon, J. *Bull. Korean Chem. Soc.* **2009**, *30*, 719; (s) Lee, H. N.; Kim, H. N.; Swamy, K. M. K.; Park, M. S.; Kim, J.; Lee, H.; Lee, K.-H.; Park, S.; Yoon, J. *Tetrahedron Lett.* **2008**, *49*, 1261; (t) Lee, Y. J.; Seo, D.; Kwon, J. Y.; Son, G.; Park, M. S.; Choi, Y.-H.; Soh, J. H.; Lee, H. N.; Lee, K. D.; Yoon, J. *Tetrahedron* **2006**, *62*, 12340; (u) Coskun, A.; Akkaya, E. U. *J. Am. Chem. Soc.* **2006**, *128*, 14474; (v) Lee, D.-N.; Kim, G.-J.; Kim, H.-J. *Tetrahedron Lett.* **2008**, *50*, 4766.
6. (a) del Campo, O.; Carbayo, A.; Cuevas, J. V.; Muñoz, Z.; García-Herbosa, G.; Moreno, D.; Ballesteros, E.; Basurto, S.; Gómez, T.; Torroba, T. *Chem. Commun.* **2008**, 4576; (b) Santra, M.; Ryu, D.; Chatterjee, A.; Ko, S.-K.; Shin, I.; Ahn, K. H. *Chem. Commun.* **2009**, 2115.
7. For recent review, see: (a) Kim, H. N.; Lee, M. H.; Kim, H. J.; Kim, J. S.; Yoon, J. *Chem. Soc. Rev.* **2008**, *37*, 1465; (b) Li, H.; Fan, J.; Wang, J.; Tian, M.; Du, J.; Sun, S.; Sun, P.; Peng, X. *Chem. Commun.* **2009**, 5904; (c) Jou, M. J.; Chen, X.; Swamy, K. M. K.; Kim, H. N.; Kim, H.-J.; Lee, S.-g.; Yoon, J. *Chem. Commun.* **2009**, 7218; (d) Zhou, Y.; Fang, W.; Kim, Y.; Kim, S.; Yoon, J. *Org. Lett.* **2009**, *11*, 4442; (e) Kwon, J. Y.; Jang, Y. J.; Lee, Y. J.; Kim, K.-M.; Seo, M.-S.; Nam, W.; Yoon, J. *J. Am. Chem. Soc.* **2005**, *127*, 10107; (f) Shiraishi, Y.; Sumiya, S.; Kohno, Y.; Hirai, T. *J. Org. Chem.* **2008**, *73*, 8571; Zheng, H.; Qian, Z.-H.; Xu, L.; Yuan, F.-F.; Lan, L.-D.; Xu, J.-G. *Org. Lett.* **2006**, *8*, 859; (g) Zhang, X.; Xiao, Y.; Qian, X. *Angew. Chem., Int. Ed.* **2008**, *47*, 8025; (h) Kou, S.; Lee, H. N.; Noort, D. v.; Swamy, K. M. K.; Kim, S. H.; Soh, J. H.; Lee, K.-M.; Nam, S.-W.; Yoon, J.; Park, S. *Angew. Chem., Int. Ed.* **2008**, *47*, 872.
8. Shi, W.; Sun, S.; Li, X.; Ma, H. *Inorg. Chem.* **2010**, *49*, 1206.
9. (a) Xu, Z.; Baek, K.-H.; Kim, H. N.; Cui, J.; Qian, X.; Spring, D. R.; Shin, I.; Yoon, J. *J. Am. Chem. Soc.* **2010**, *132*, 601; (b) Chen, X.; Ko, S.-K.; Kim, M. J.; Shin, I.; Yoon, J. *Chem. Commun.* **2010**, 46, 2751; (c) Swamy, K. M. K.; Ko, S.-K.; Kwon, S. K.; Lee, H. N.; Mao, C.; Kim, J.-M.; Lee, K.-H.; Kim, J.; Shin, I.; Yoon, J. *Chem. Commun.* **2008**, 5915.